Experimental and Clinical Endocrinology & Diabetes

Reprint
Volume 113, 2005

J. A. Barth Verlag
in Georg Thieme Verlag KG
Rüdigerstraße 14
70469 Stuttgart, Germany
www.thieme-connect.com
www.thieme.de/eced

Conclusions

Our goal was to quantitatively assess the binding properties of K14D10 IgG and its Fab, in terms of their ability to track beta cell mass *in vivo*. Recombinant Fab and IgG of K14D10 showed similar affinity, binding site number, and cellular specificity, supporting the feasibility of using Fabs. In addition, the affinity and binding site number of the Fab appeared to be high enough to overcome the signal emanating from unbound antibody in the extracellular fluid. However, the Fab had a reduced retention by the beta cell, and the specificity of K14D10 IgG and rFab were significantly lower than what is needed to for successful detection of beta cell mass. The *in vivo* biodistribution studies bore out these predictions made on the basis of *in vitro* screening assays, further validating its utility in evaluating molecules and their properties that will lead to an increased chance of success, and pointing to the need to develop new antibodies with higher binding specificity for beta cells.

Acknowledgements

This study has been supported by the Juvenile Diabetes Foundation International (1–2001–873) and the National Institute of Health (grants DK26190, DK53004, DK58512, and P01 DK17047), and a Career Development Award from the American Diabetes Association for CSH. Special thanks to Dr. Åke Lernmark for scientific input and helpful comments regarding the manuscript.

References

[1] Adams GP, Schier R. Generating improved single-chain Fv molecules for tumor targeting. J Immunol Methods 1999; 231: 249–260

[2] Asfari M, Janjic D, Meda P, Li G, Halban PA, Wollheim CB. Establishment of 2-mercaptoethanol-dependent differentiated insulin-secreting cell lines. Endocrinology 1992; 130: 167–178

[3] Bazin-Redureau MI, Renard CB, Scherrmann JM. Pharmacokinetics of heterologous and homologous immunoglobulin G, F(ab')2 and Fab after intravenous administration in the rat. J Pharm Pharmacol 1997; 49: 277–281

[4] Boyle CC, Paine AJ, Mather SJ. The mechanism of hepatic uptake of a radiolabelled monoclonal antibody. Int J Cancer 1992; 50: 912–917

[5] Brinkmann U, Webber K, Di Carlo A, Beers R, Chowdhury P, Chang K, Chaudhary V, Gallo M, Pastan I. Cloning and expression of the recombinant FAb fragment of monoclonal antibody K1 that reacts with mesothelin present on mesotheliomas and ovarian cancers. Int J Cancer 1997; 71: 638–644

[6] Buschard K, Brogren CH, Ropke C, Rygaard J. Antigen expression of the pancreatic beta-cells is dependent on their functional state, as shown by a specific, BB rat monoclonal autoantibody IC2. Apmis 1988; 96: 342–346

[7] Camera L, Kinuya S, Garmestani K, Pai LH, Brechbiel MW, Gansow OA, Paik CH, Pastan I, Carrasquillo JA. Evaluation of a new DTPA-derivative chelator: comparative biodistribution and imaging studies of 111In-labeled B3 monoclonal antibody in athymic mice bearing human epidermoid carcinoma xenografts. Nucl Med Biol 1993; 20: 955–962

[8] Carter P, Kelley RF, Rodrigues ML, Snedecor B, Covarrubias M, Velligan MD, Wong WL, Rowland AM, Kotts CE, Carver ME et al. High level Escherichia coli expression and production of a bivalent humanized antibody fragment. Biotechnology (NY) 1992; 10: 163–167

[9] Casey JL, Napier MP, King DJ, Pedley RB, Chaplin LC, Weir N, Skelton L, Green AJ, Hope-Stone LD, Yarranton GT, Begent RH. Tumour targeting of humanised cross-linked divalent-Fab' antibody fragments: a clinical phase I/II study. Br J Cancer 2002; 86: 1401–1410

[10] Colcher D, Bird R, Roselli M, Hardman KD, Johnson S, Pope S, Dodd SW, Pantoliano MW, Milenic DE, Schlom J. In vivo tumor targeting of a recombinant single-chain antigen-binding protein. J Natl Cancer Inst 1990; 82: 1191–1197

[11] Colcher D, Pavlinkova G, Beresford G, Booth BJ, Choudhury A, Batra SK. Pharmacokinetics and biodistribution of genetically-engineered antibodies. Q J Nucl Med 1998; 42: 225–241

[12] Covell DG, Barbet J, Holton OD, Black CD, Parker RJ, Weinstein JN. Pharmacokinetics of monoclonal immunoglobulin G1, F(ab')2, and Fab' in mice. Cancer Res 1986; 46: 3969–3978

[13] DeNardo SJ, Peng JS, DeNardo GL, Mills SL, Epstein AL. Immunochemical aspects of monoclonal antibodies important for radiopharmaceutical development. Int J Rad Appl Instrum B 1986; 13: 303–310

[14] Garnuszek P, Licinska I, Fiedor P, Mazurek AP. The synthesis, radioiodination and preliminary biological study of the new carboxylic derivatives of dithizone. Appl Radiat Isot 1998; 49: 1563–1571

[15] Hampe CS, Lundgren P, Daniels TL, Hammerle LP, Marcovina SM, Lernmark A. A novel monoclonal antibody specific for the N-terminal end of GAD65. J Neuroimmunol 2001; 113: 63–71

[16] Izard ME, Boniface GR, Hardiman KL, Brechbiel MW, Gansow OA, Walkers KZ. An improved method for labeling monoclonal antibodies with samarium-153: use of the bifunctional chelate 2-(p-isothiocyanatobenzyl)-6- methyldiethylenetriaminepentaacetic acid. Bioconjug Chem 1992; 3: 346–350

[17] Kabat EA, Wu TT, Perry HM, Gottesman K, Foeller C. Sequences of Proteins of Immunological Interest. Washington, DC: Services US DoHaH, 1991

[18] Konidaris C, Simonson W, Michelsen B, Papadopoulos GK. Specific monoclonal antibodies against the surface of rat islet beta cells. Cell Biol Int 2002; 26: 817–828

[19] Logsdon CD, Moessner J, Williams JA, Goldfine ID. Glucocorticoids increase amylase mRNA levels, secretory organelles, and secretion in pancreatic acinar AR42J cells. J Cell Biol 1985; 100: 1200–1208

[20] Malaisse WJ. On the track to the beta-cell. Diabetologia 2001; 44: 393–406

[21] Milenic DE, Yokota T, Filpula DR, Finkelman MA, Dodd SW, Wood JF, Whitlow M, Snoy P, Schlom J. Construction, binding properties, metabolism, and tumor targeting of a single-chain Fv derived from the pancarcinoma monoclonal antibody CC49. Cancer Res 1991; 51: 6363–6371

[22] Moore A, Bonner-Weir S, Weissleder R. Noninvasive in vivo measurement of beta-cell mass in mouse model of diabetes. Diabetes 2001; 50: 2231–2236

[23] Mossner J, Logsdon CD, Williams JA, Goldfine ID. Insulin, via its own receptor, regulates growth and amylase synthesis in pancreatic acinar AR42J cells. Diabetes 1985; 34: 891–897

[24] Neidhardt FC, Bloch PL, Smith DF. Culture medium for enterobacteria. J Bacteriol 1974; 119: 736–747

[25] Padoa CJ, Banga JP, Madec AM, Ziegler M, Schlosser M, Ortqvist E, Kockum I, Palmer J, Rolandsson O, Binder KA, Foote J, Luo D, Hampe CS. Recombinant Fabs of human monoclonal antibodies specific to the middle epitope of GAD65 inhibit type 1 diabetes-specific GAD65Abs. Diabetes 2003; 52: 2689–2695

[26] Sweet IR, Cook DL, Lernmark A, Greenbaum CJ, Krohn KA. Non-invasive imaging of beta cell mass: a quantitative analysis. Diabetes Technol Ther 2004 b; 6: 652–659

[27] Sweet IR, Cook DL, Lernmark A, Greenbaum CJ, Wallen AR, Marcum ES, Stekhova SA, Krohn KA. Systematic screening of potential beta-cell imaging agents. Biochem Biophys Res Commun 2004 a; 314: 976–983

[28] Viti F, Tarli L, Giovannoni L, Zardi L, Neri D. Increased binding affinity and valence of recombinant antibody fragments lead to improved targeting of tumoral angiogenesis. Cancer Res 1999; 59: 347–352

[29] Yokota T, Milenic DE, Whitlow M, Wood JF, Hubert SL, Schlom J. Microautoradiographic analysis of the normal organ distribution of radioiodinated single-chain Fv and other immunoglobulin forms. Cancer Res 1993; 53: 3776–3783

[30] Ziegler B, Lucke S, Kohler E, Hehmke B, Schlosser M, Witt S, Besch W, Ziegler M. Monoclonal antibody-mediated cytotoxicity against rat beta cells detected in vitro does not cause beta-cell destruction in vivo. Diabetologia 1992; 35: 608–613

In Vitro and *In Vivo* Evaluation of Novel Glibenclamide Derivatives as Imaging Agents for the Non-Invasive Assessment of the Pancreatic Islet Cell Mass in Animals and Humans

S. Schneider[1*], P. J. Feilen[2]
M. Schreckenberger[3]
M. Schwanstecher[4]
C. Schwanstecher[4], H. G. Buchholz[3]
O. Thews[5], K. Oberholzer[6]
A. Korobeynikov[7], A. Bauman[7]
S. Comagic[7], M. Piel[7]
E. Schirrmacher[3*], C. Y. Shiue[8]
A. A. Alavi[8], P. Bartenstein[3]
F. Rösch[7], M. M. Weber[2]
H. H. Klein[1], R. Schirrmacher[3]

Abstract

Pancreatic islet cell mass (PICM) is a major determinant of the insulin secretory capacity in humans. Currently, the only method for accurate assessment of the PICM is an autopsy study. Thus, development of a technique allowing the non-invasive quantification of PICM is of great interest. The aim of this study was to develop such a non-invasive technique featuring novel fluorine- and ^{99m}Tc-labelled glibenclamide derivatives. Despite the structural modifications necessary to introduce fluorine into the glibenclamide molecule, all derivatives retained insulin stimulating capacity as well as high affinity binding to human SUR1 when compared to the original glibenclamide. Contrastingly, the lipophilicity of the fluorine-labelled derivatives was altered depending on the particular modification. In the human PET-study a constant but weak radioactive signal could be detected in the pancreas using a fluorine-labelled glibenclamide derivative. However, a reliable assessment and visualisation of the PICM could not be obtained. It can be assumed that the high uptake of the fluorine-labelled tracer e.g. into the the liver and the high plasma protein binding leads to a relatively low signal-to-noise ratio. In case of the presented fluorine-labelled glibenclamide based compounds this could be the result of their invariably high lipophilicity. The development of a ^{99m}Tc-labelled glibenclamide derivative with a lower lipophilicity and differing *in vivo* behaviour, glibenclamide based compounds for non-invasive imaging of the pancreatic islet cell mass may be possible.

Key words
Glibenclamide derivatives · pancreatic islet cell mass · sulfonylurea receptor 1

Introduction

The non-invasive assessment of the pancreatic islet cell mass (PICM) *in vivo* would be of great medical interest but there is currently no technique available. In type 1 diabetic patients, the chronic and progressive loss of the insulin producing pancreatic islet cells due to autoimmune destruction has led to concerted efforts to prevent further loss of β-cells by autoantigen-specific immunotherapy of pre-diabetic patients (Bottino et al., 2003). With a non-invasive technique, the effect of different interven-

Affiliation
[1] Medical Department I, University Hospital Bergmannsheil, University of Bochum, Bochum, Germany
[2] Division of Endocrinology and Metabolism, I. Medical Department, University of Mainz, Mainz, Germany
[3] Department of Nuclear Medicine, University of Mainz, Mainz, Germany
[4] Institute of Pharmacology and Toxicology, University of Braunschweig, Braunschweig, Germany
[5] Institute of Physiology and Pathophysiology, University of Mainz, Mainz, Germany
[6] Department of Radiology, University of Mainz, Mainz, Germany
[7] Institute of Nuclear Chemistry, University of Mainz, Mainz, Germany
[8] Department of Radiology, University of Pennsylvania, Philadelphia, USA

* Both authors contributed equally.

Correspondence
Dr. Stephan Schneider · Medical Department I · University Hospital Bergmannsheil · Bürkle-de-la-Camp-Platz 1 · 44789 Bochum · Germany · T + 49 23 43 02 34 69 · F + 49 23 43 02 64 03 · E-mail: Stephan.Schneider@ruhr-uni-bochum.de

Received: July 6, 2004 · **First decision:** September 20, 2004 · **Accepted:** May 2, 2005

Bibliography
Exp Clin Endocrinol Diabetes 2005; 113: 388 – 395 © J. A. Barth Verlag in Georg Thieme Verlag KG · Stuttgart · New York ·
DOI 10.1055/s-2005-865711 ·
ISSN 0947-7349

tion strategies could be easily monitored. Furthermore, the longitudinal monitoring of the PICM of patients with type 2 diabetes mellitus under different antidiabetic therapies (e.g. GLP-agonists) may lead to the development of new strategies for treatment.

Insulin secretion is regulated by the membrane potential of the β-cell, which depends on the activity of ATP-sensitive K^+ channels (K_{ATP} channels) in the plasma membrane. Closure of K_{ATP} channels due to a rise of the cytoplasmic ATP/ADP ratio results in a depolarisation of the membrane and in the opening of voltage-sensitive Ca^{2+} channels. The increase in cytoplasmic Ca^{2+} stimulates the exocytosis of insulin. K_{ATP} channels are composed of a small inwardly rectifying K^+ channel subunit (Kir6.1 or Kir6.2) plus a sulfonylurea receptor (SUR) belonging to the ATP-binding cassette superfamily (Aguilar-Bryan and Bryan, 1999). SURs represent the target for hypoglycemic sulfonylureas (e.g. glibenclamide, tolbutamide), a group of well known antidiabetic agents which have been in clinical use for years for the treatment of type 2 diabetic patients (Proks et al., 2002). So far, three sulfonylurea receptors have been cloned: SUR1, SUR2A, and SUR2B. While SUR1 is expressed in a very high density at the internal face of the plasma membrane (Schwanstecher et al., 1994; Uhde et al., 1999) of the pancreatic islet cells (glucagon-secreting α- and insulin secreting β-cells) but not in the exocrine part of the pancreas, the SUR2 isoforms are predominant in cardiac, skeletal, and smooth muscle cells (Aguilar-Bryan and Bryan, 1999). Therefore, a radio-labelled glibenclamide derivative could be a feasible tracer for visualizing the PICM in humans by accumulation at the internal face of the plasma membrane of pancreatic islet cells due to binding to SUR1 and estimation of the specific radioactivity over regions of interest (e.g. pancreas) using positron emission tomography (PET) or single photon emission computed tomography (SPECT). As radioactive labelling with fluorine-18 or technetium-99m could alter the biological behaviour of the derivative (binding affinity, lipophilicity etc.), we synthesised and evaluated different labelled tolbutamide derivatives (Shiue et al., 2001; Schirrmacher et al., 2002). For several reasons (overall radiochemical yield, binding affinity, deposition time at the receptor etc.) none of them was suitable for *in vivo* evaluations. Therefore, the intention of this study is to demonstrate that fluorine- and ^{99m}Tc-labelled glibenclamide derivatives could be synthesised *de novo* with well preserved biological activity and to investigate whether they might serve as potential tracers for non-invasive visualisation of the PICM.

Material and Methods

Chemistry and radiochemistry

Our search for potential tracers for the visualization of the PICM (Shiue et al., 2004; Schirrmacher et al., 2002; Shiue et al., 2001) led us to the *de novo* syntheses of twenty different fluorine-labelled glibenclamide derivatives (Fig. **1a** and Table **1a**) and a Renium (Re) labelled glibenclamide derivative (Table **1b**). Exact syntheses of all derivatives will be described elsewhere. For *in vivo* evaluations 2-[^{18}F]fluoroethoxy-5-bromoglibenclamide (compound 9 in Table **1a**) was chosen due to its well preserved insulin stimulating capacity, the high binding affinity to human SUR1 and the relatively low logD (cf. results). In another *in vivo*

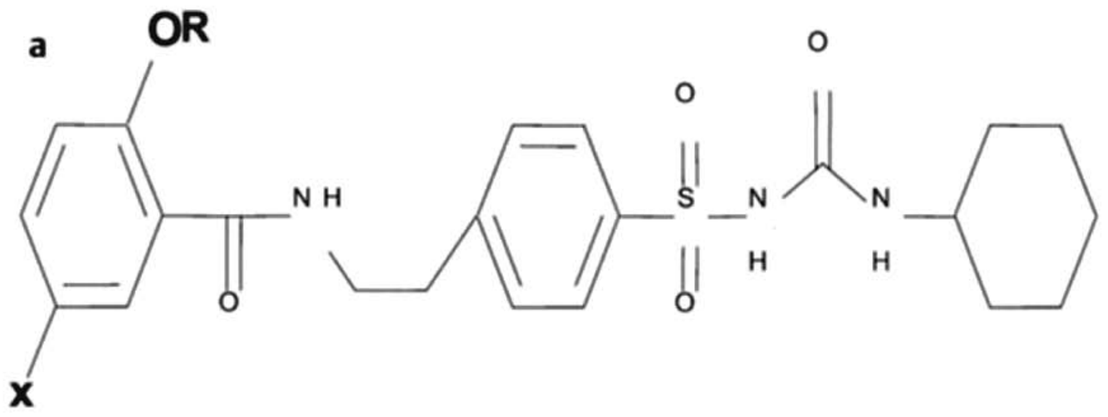

Fig. **1a** Structure of all synthesised fluorine-labelled glibenclamide derivatives (compounds 1–20) and the original glibenclamide (org. glib., see also Table **1a**).

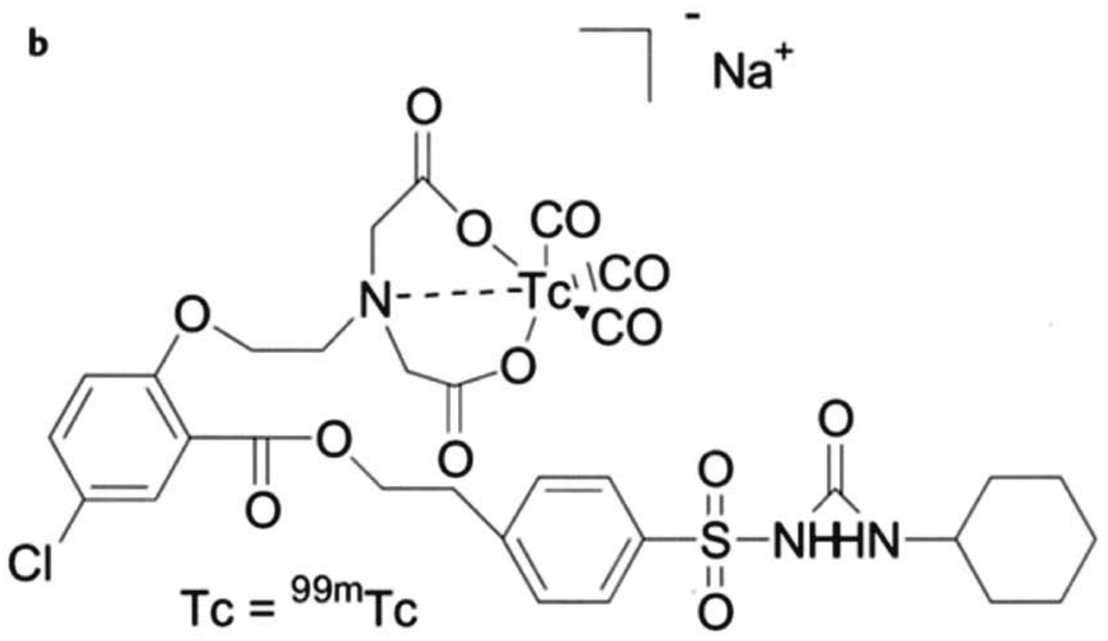

Fig. **1b** Structure of the ^{99m}Tc-labelled glibenclamide derivative.

approach the ^{99m}Tc-labelled glibenclamide derivative (radioactive analogue of the Renium-labelled derivative) was used, due to its significant lower lipophylicity (Fig. **1b**).

The radiolabelling was performed using 2-[^{18}F]fluoroethyltosylate as an intermediate as described in the literature (Shiue et al., 2001) in an overall radiochemical yield of 10% (referring to the starting activity of [^{18}F]fluoride). Briefly, no-carrier-added (nca) [^{18}F]fluoride prepared by the ^{18}O(p,n)^{18}F nuclear reaction on an enriched water (95% + ^{18}O) target was added to a solution of potassium carbonate/Kryptofix 2.2.2. in a Pyrex vessel. The water was evaporated using a stream of nitrogen at 80 °C and co-evaporated to dryness with acetonitrile (2 × 1 ml). A solution of ethylene glycol di-*p*-tosylate (5 mg in 0.5 ml of acetonitrile) was added to the dried K[^{18}F] and the solution was heated at 80 °C for 5 min. The crude 2-[^{18}F]fluoroethyltosylate was purified by HPLC (LiChrospher RP18 5EC, 250 × 10 mm, eluent: acetonitrile/water 1/1 [v/v], flow: 5 ml/min retention time 10–12 min), loaded on a SepPak C-18 solid phase cartridge and eluted with diethylether (2 ml). A solution of *N*-(4-[β-{2-hydroxy-5-bromobenzenecarboxamido}ethyl]benzenesulfonyl)-*N'*-cyclohexylurea (21) (1 mg, 1.9 µmol) and 1 N NaOH (7 µl) in DMSO (250 µl) were added to the 2-[^{18}F]fluoroethyltosylate solution. The mixture was heated at 80 °C for 3 min and then at 120 °C for additional 10 min. The crude product (compound 22) was injected into an isocratic HPLC system (LiChrospher RP18 5EC 250 × 10 mm, flow: 4 ml/min, eluent: acetonitrile/0.5 M ammonia acetate buffer (52/48) (v/v)) and the fraction containing compound 22 (R_t = 21 min) was collected, diluted with water (20 ml), and loaded onto a SepPac C-18 solid phase cartridge. The cartridge was dried in a stream of nitrogen, eluted with 1 ml of ethanol and diluted with 10 ml of physiological saline. After sterile filtration, the final ster-

Table **1 a** Structure of all synthesised fluorine-labelled glibenclamide derivatives (compounds 1 – 20) and the original glibenclamide (org. glib., see also Fig. **1 a**). Furthermore, the data shown here represent the estimated lipophilicity (LogD), the dissociation constants (K_{Ds}), the half-maximally inhibitory drug-concentrations (IC_{50} values), the Hill coefficients and insulin stimulating capacity (stimulation index) of all analogous non-radioactive ^{19}F-glibenclamide derivatives compared to the original glibenclamide. Results are mean ± SEM. 4 – 6 experiments

Compound Nr.	*x*	*R*	*logD*	*K_d (nM)*	*IC_{50} (nM)*	*Hill coefficient*	*Stimulation index*
orig. glib.	Cl	CH_3	1.74	0.33 ± 0.02	0.63 ± 0.04	1.00	3.3 ± 0.4
1	F	CH_2CH_2F	1.45	–	–	–	3.6 ± 0.9
2	F	$CH_2CH_2CH_2F$	1.52	–	–	–	3.5 ± 0.5
3	F	$CH_2CH_2CH_2CH_2F$	1.62	–	–	–	3.3 ± 0.5
4	F	$CH_2(C_6H_4)F$	1.93	0.55 ± 0.11	1.14 ± 0.23	0.92 ± 0.04	3.2 ± 0.3
5	Cl	CH_2CH_2F	1.67	–	–	–	3.6 ± 0.5
6	Cl	$CH_2CH_2CH_2F$	1.76	0.22 ± 0.03	0.43 ± 0.06	0.98 ± 0.02	3.5 ± 0.4
7	Cl	$CH_2CH_2CH_2CH_2F$	1.97	0.19 ± 0.02	0.36 ± 0.04	0.92 ± 0.03	3.9 ± 0.6
8	Cl	$CH_2(C_6H_4)F$	2.22	0.25 ± 0.03	0.52 ± 0.06	1.04 ± 0.03	3.3 ± 0.7
9	Br	CH_2CH_2F	1.69	0.22 ± 0.03	0.41 ± 0.02	0.92 ± 0.04	3.3 ± 0.5
10	Br	$CH_2CH_2CH_2F$	1.88	0.20 ± 0.01	0.39 ± 0.02	0.92 ± 0.02	3.4 ± 0.5
11	Br	$CH_2CH_2CH_2CH_2F$	2.00	0.24 ± 0.02	0.45 ± 0.04	1.06 ± 0.03	3.1 ± 0.9
12	Br	$CH_2(C_6H_4)F$	2.34	0.24 ± 0.01	0.50 ± 0.03	1.02 ± 0.04	3.2 ± 0.4
13	I	CH_2CH_2F	1.81	–	–	–	3.6 ± 0.5
14	I	$CH_2CH_2CH_2F$	2.01	–	–	–	3.2 ± 0.3
15	I	$CH_2CH_2CH_2CH_2F$	2.12	–	–	–	3.0 ± 0.7
16	I	$CH_2(C_6H_4)F$	2.38	0.28 ± 0.02	0.57 ± 0.04	0.96 ± 0.03	3.4 ± 0.4
17	H	CH_2CH_2F	1.31	–	–	–	3.8 ± 0.7
18	H	$CH_2CH_2CH_2F$	1.35	–	–	–	3.3 ± 0.7
19	H	$CH_2CH_2CH_2CH_2F$	1.50	–	–	–	3.2 ± 0.4
20	H	$CH_2(C_6H_4)F$	1.80	1.37 ± 0.25	2.83 ± 0.51	0.91 ± 0.04	3.0 ± 0.4

Table **1 b** The data shown here represent estimated lipophilicity (logD), the dissociation constant (K_D), the half-maximally inhibitory drug-concentration (IC_{50} value), the Hill coefficient and insulin stimulating capacity (stimulation index) of the analogous non-radioactive Re-glibenclamide derivative. Results are mean ± SEM. 4 – 6 experiments

Compound	*logD*	*K_D (nM)*	*IC_{50} (nM)*	*Hill coefficient*	*Stimulation index*
Re glib.	– 0.2	0.5 ± 0.04	0.99 ± 0.05	1.1	3.5 ± 0.7

ile product was obtained as a 10% ethanolic saline solution for injection in an overall radiochemical yield of 8 – 10% in a synthesis time of 110 min from EOB. The specific activity was 50 – 60 GBq/µmol.

Isolation of rat islets of Langerhans

The islet isolations were performed according to the procedures as described before (Schneider et al., 2005 Schneider et al., 2003). In brief, for each assay, 6 Sprague Dawley rats (Central Animal Facility, University of Mainz), 8 weeks old, body weight 280 – 330 g, were used as islet donors. Rats were anaesthetised by intraperitoneal pentobarbital administration (60 mg/kg), a midline abdominal incision was performed, and the pancreas was exposed and injected via the pancreatic duct with Hanks' balanced salt solution (HBSS; Gibco BRL, Long island, NY) containing 1.7 mg/ml collagenase (Serva PanPlus, Heidelberg, Germany). After sacrifice of the animal, the pancreatic tissue was surgically removed and incubated for 10 min at 37 °C in the collagenase solution. Mechanical disruption of the digested pancreatic tissue was achieved by further incubation in collagenase solution at 37 °C for 10 min, interrupted every 2 min by shaking for 30 s. Digestion was stopped by addition of 4 °C HBSS plus 10% fetal calf serum (FCS). Islet purification was achieved using a discontinuous three-phase Ficoll density gradient (densities: 1.090, 1.077, and 1.040).

Insulin secretion studies

These studies were performed according to the procedures as described previously (Wängler et al., 2004 a, b; Schirrmacher et al., 2002). Ten islets of equal size and shape were hand-picked

and transferred into a culture-insert (membrane pore diameter 12 µm; Millicell PCF, Millipore, France). The inserts were placed into a well of a 24-well culture plate (Falcon Multiwell, Becton Dickinson, USA). First, the basal insulin secretion was estimated by incubating the islets in normoglycemic culture-medium (RPMI 1640 + D-glucose 1 g/l + 10% FCS) for 1 hour at 37 °C. Afterwards, the inserts with the islets were transferred into normoglycemic culture-medium (RPMI 1640 + D-glucose 1 g/l + 10% FCS) containing 50 nmol/l of the original glibenclamide or the derivatives and incubated for a stimulation period of 1 hour. At the end of the incubation period, insulin levels were measured by the rat-insulin ELISA purchased from Mercodia (Uppsala, Sweden). The insulin secretion of the islets was expressed as insulin release per islet/h. The stimulation index was calculated by dividing the insulin output from the stimulation period by insulin secretion during the basal incubation.

Binding affinities for human SUR1

[^{3}H]glibenclamide (specific activity ~1.9 GBq/µmol) was purchased from NEN (Dreieich, Germany). Stock solutions of all drugs were prepared in either KOH (50 mM) or dimethyl sulfoxide with a final solvent concentration in the media below 1%. Transfections and membrane preparations were performed as described (Schwanstecher et al., 1992; Schwanstecher et al., 1998). Briefly, COS-1 cells, cultured in DMEM HG (10 mM glucose) supplemented with 10% FCS, were plated at a density of 5×10^5 cells per dish (94 mm), and allowed to attach overnight. 200 µg of pECE-human SUR1 complementary DNA (GenBank NP_000343) were used to transfect 10 plates. For transfection, the cells were incubated 4 hours in a Tris-buffered salt solution containing DNA (5 – 10 µg/ml) plus DEAE-dextran (1 mg/ml), 2 min in HEPES-buffered salt solution plus dimethyl sulfoxide (10%), and 4 hours in DMEM-HG plus chloroquine (100 µM). Cells were then returned to DMEM-HG plus 10% FCS and were used 60 – 72 hours post transfection to prepare membranes as described (Schwanstecher et al., 1992). To measure binding to membranes from COS-cells, the resuspended fraction (final protein concentration 5 – 50 µg/ml) was incubated in "Tris-buffer" (50 mM, pH 7.4) containing [^{3}H]glibenclamide (final concentration 0.3 nM), nonspecific binding was determined with 1 µM glibenclamide and displacing drugs as described. Incubations were carried out for 1 h at room temperature and were terminated by rapid filtration through Whatman GF/B filters. Half-maximally inhibitory drug-concentrations (IC_{50} values) and Hill coefficients (n) were estimated by fitting the function $B = 1/(1 + [drug/IC_{50}]^n)$ to the data of each single diplacement experiment. K_Ds were calculated from IC_{50} values as described (Schwanstecher et al., 1992).

Estimation of the lipophilicity

The logD values of the original glibenclamide and the glibenclamide derivatives were estimated according the "OECD Guideline for testing of chemicals" with the HPLC method (Eadsforth and Moser, 1983; Eadsforth, 1986).

Biodistribution studies in rats

2-[^{18}F]fluoroethoxy-5-bromoglibenclamide (n = 4) or ^{99m}Tc-labelled glibenclamide (n = 3) were injected intravenously in rats at a mean activity of 15 MBq. At different time points, the animals were sacrificed and the organs including the pancreas were removed (dried organs without any obvious blood contamination), weighed, and assayed for radioactivity, and corrected for decay. All experiment protocols have been approved by the regional animal ethics committee and were conducted according to German federal law.

Imaging protocol (PET, MRI, and PET/MRI-overlay)

Two healthy subjects underwent a PET scan at the Department of Nuclear Medicine of the University Hospital Mainz on a Siemens ECAT EXACT PET scanner (Siemens/CTI, Erlangen, Germany). After abdomen sonography and epicutaneous marking of the pancreas position, the subjects were placed in the PET scanner with the pancreas within the field-of-view (16.2 cm). After a 10-min transmission scan with a ^{68}Ga/Ge ring source, 98 MBq (subject 1) and 118 MBq (subject 2) of 2-[^{18}F]fluoroethoxy-5-bromoglibenclamide were injected intravenously.

Simultaneously with the tracer injection, a dynamic PET scan using three-dimensional (3D) acquisition mode started with the following frames: 2 min × 10 frames and subsequently 5 min × 8 frames. After the abdomen scan, a static whole-body scan (skull base – proximal femora) and a brain scan were performed in 3D acquisition mode in order to image whole-body tracer distribution. Correction for dead time, scatter, and random coincidence were applied, and the dynamic images were reconstructed using iterative reconstruction algorithm (OSEM) with a 6-mm Gaussian filter. The static whole-body data were reconstructed using filtered back-projection with a 6-mm Hamming filter. For the reconstruction of the brain images, a filtered back-projection algorithm with 4-mm Hamming filter was used with mathematical attenuation correction.

Magnetic resonance imaging (MRI) was performed on another day with a 1.5-T system (Magnetom Sonata, Siemens Medical Systems, Erlangen, Germany). At first, transversal T1- and T2-weighted images were acquired. For dynamic acquisition, T1-weighted flash 2D sequences with fat supression were applied. After obtaining unenhanced images, we obtained four enhanced series, starting 26 s after the initiation of IV bolus injection of 0.1 mL/kg gadolinium-DTPA (Magnevist, Schering, Berlin, Germany).

The quantitative analysis of the dynamic tracer distribution in the liver and in the pancreas were performed using regions-of-interest (ROI) which were manually drawn in the 3D MRI data and superimposed onto the realigned PET data. For MRI/PET realignment and image fusion, the MPI Tool software was used (Pietrzyk et al., 1994; Pietrzyk et al., 1990).

Statistics

Values are given as mean ± standard error of mean (SEM). Statistical significance of differences was calculated with an unpaired Student's *t*-test (two-sided).

Results

Evaluation of the insulin stimulating capacity

Six groups of ten islets were incubated for 60 min with either 50 nmol/l of glibenclamide or the glibenclamide derivatives. It

was interesting to note that although the chemical structure of the glibenclamide molecule was modified at different sites and in different ways, none of the derivatives showed an insulin stimulating capacity significantly different to that of the original glibenclamide (Tables **1 a** and **1 b**).

Binding affinities for human SUR1

Competition binding experiments were performed to assess the binding affinity of the glibenclamide derivatives towards human SUR1 (Tables **1 a** and **1 b**). The results showed that similar to unlabelled glibenclamide, all tested glibenclamide derivatives (compounds 4, 6 – 12, 16, 20 and the Re-labelled glibenclamide) induced a complete monophasic inhibition curve with Hill coefficients close to 1 (range 0.91 – 1.1) yielding dissociation constants (K_{Ds}) of 0.19 to 0.55 nM. The corresponding values for glibenclamide were 1.0 (Hill coefficient) and 0.33 (K_D value) (Table **1 a**). In conclusion, all *de novo* synthesised derivatives showed a rather high affinity toward human SUR1 irrespective of the introduced structural elements.

Determination of the lipophilicity

The lipophilicity (logD) of the fluorine-labelled derivatives could be altered, dependent on the modifications introduced (Table **1 a**). For example, derivatives 8, 12, and 16 were found to be much more lipophilic due to features such as the fluorobenzyl moiety and the chlorine, bromine, and iodine substituents. This observation could be of interest because lipophilic ligands show in some cases an unspecific uptake by different organs e.g. the liver and this could lead to resolution problems. Therefore, in the case of the fluorine-labelled derivatives the decision was in favour for 2-[^{19}F]fluoroethoxy-5-bromoglibenclamide (compound 9 in Table **1 a**) because the ligand seems to be less lipophilic compared to most of the other synthesised fluorine-labelled compounds, the affinity to human SUR1 was rather high (K_D of 0.22 ± 0.03) and the radioactive label could be easily introduced. Furthermore, based on the above mentioned considerations we used the *de novo* synthesised ^{99m}Tc-labelled glibenclamide derivative for *in vivo* evaluation, because the analogous non-radioactive Re-derivative showed a 20-fold lower lipophilicity with a logD of – 0.2 (Table **1 b**), compared to all tested fluorine-labelled derivatives (Table **1 a**).

Biodistribution studies of 2-[^{18}F]fluoroethoxy-5-bromoglibenclamide and ^{99m}Tc-glibenclamide

Tissue distribution of 2-[^{18}F]fluoroethoxy-5-bromoglibenclamide in rats (Fig. **2 a**) showed that pancreatic tissue displayed a weak but near constant accumulation of the tracer with 0.084 ± 0.01 % of the injected dose per gram (%ID/g) after 5 min and only a slight decrease after 60 min. In contrast, the tracer accumulation in the liver was approximately 100-fold higher compared to the pancreas uptake. The tracer uptake in the kidney and the plasma protein binding was also rather high, whereas the brain uptake was very low.

In contrast, the tissue distribution of ^{99m}Tc-labelled glibenclamide was complete different (Fig. **2 b**). The liver uptake of the tracer was 1000-fold and the plasma protein binding 2500-fold lower, whereas the pancreas uptake was only slighthly reduced (10-fold) when compared with 2-[^{18}F]fluoroethoxy-5-bromoglibenclamide at 1 h after tracer application. These preliminary results are encouraging but more work is needed to prove if a ^{99m}Tc-labelled glibenclamide derivative will really lead to a better signal to noise ratio.

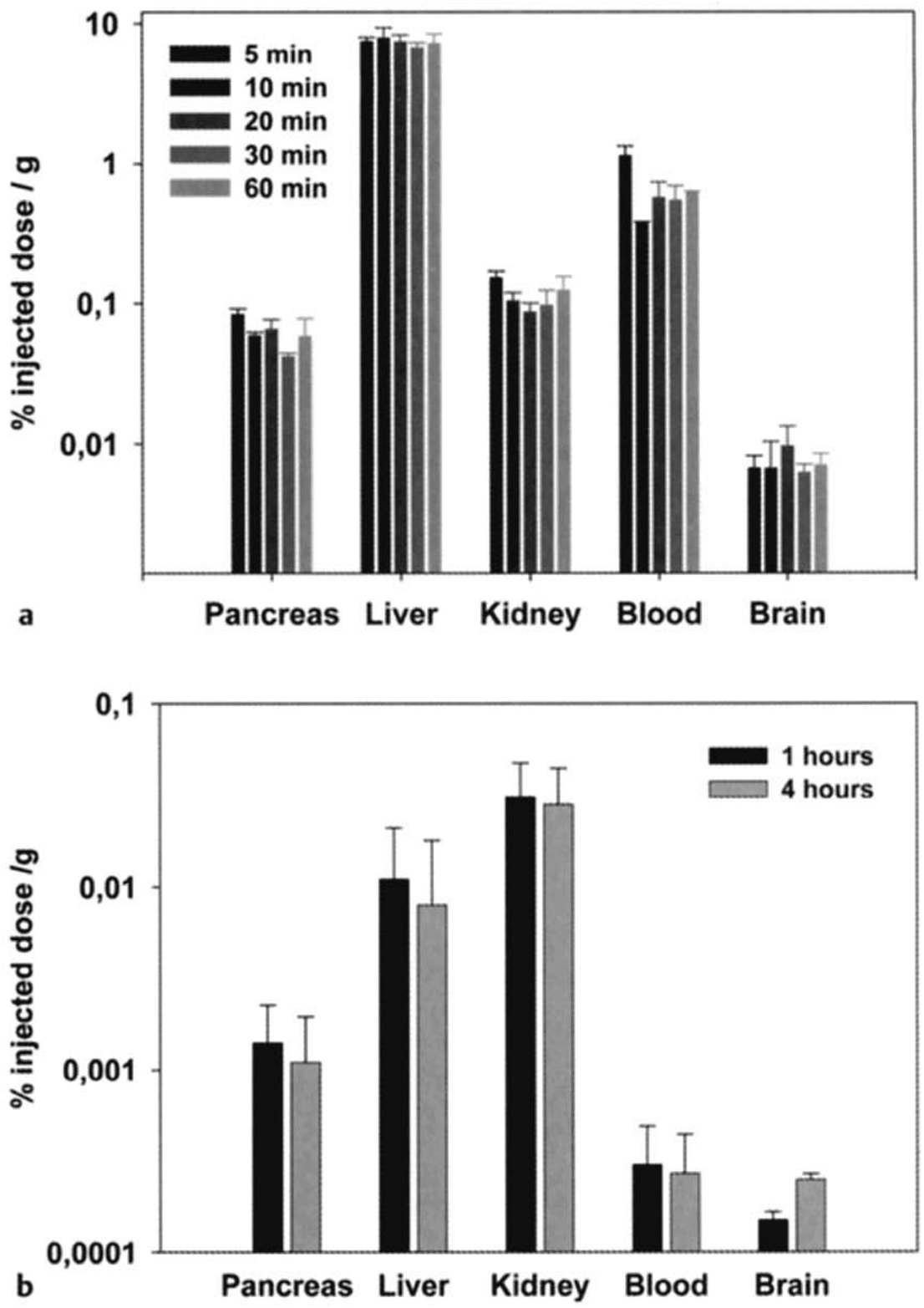

Fig. **2 a** and **b** **a** Biodistribution of 2-[^{18}F]fluoroethoxy-5-bromoglibenclamide in normoglycemic rats (n = 4). **b** Biodistribution of ^{99m}Tc-labelled glibenclamide in normoglycemic rats (n = 3). Data are %ID/g of tissue. Results shown as mean ± SEM.

First attempt to visualize the pancreatic islet cell mass in humans with a positron-emitter labelled glibenclamide derivative using positron emission tomography

The dynamic PET scans of the two male healthy volunteers showed a slight uptake and constant retention of 2-[^{18}F]fluoroethoxy-5-bromoglibenclamide in the pancreas during the examination time of 0 – 60 min p.i. As an example, the hepatic and pancreatic tracer distribution of one subject is shown in Fig. **3**. The relative uptake of the tracer in the liver (in Bq/cm^2) was approximately 10-fold higher than in the pancreas. The time activity curves of the liver showed a relatively fast uptake, plateau at 45 min p.i., and a very slow washout. In the pancreas, after an initial fast uptake, there was a slow activity increase up to the end of the dynamic scan (60 min p.i.). Probably the high lipophilicity of the tracer, the consecutive high uptake into the liver and the high plasma protein binding lead to a poor signal-to-noise ratio. Thus a good detection of the pancreatic signal was not achieved and so far a visualisation of the PICM has failed (Fig. **4**).

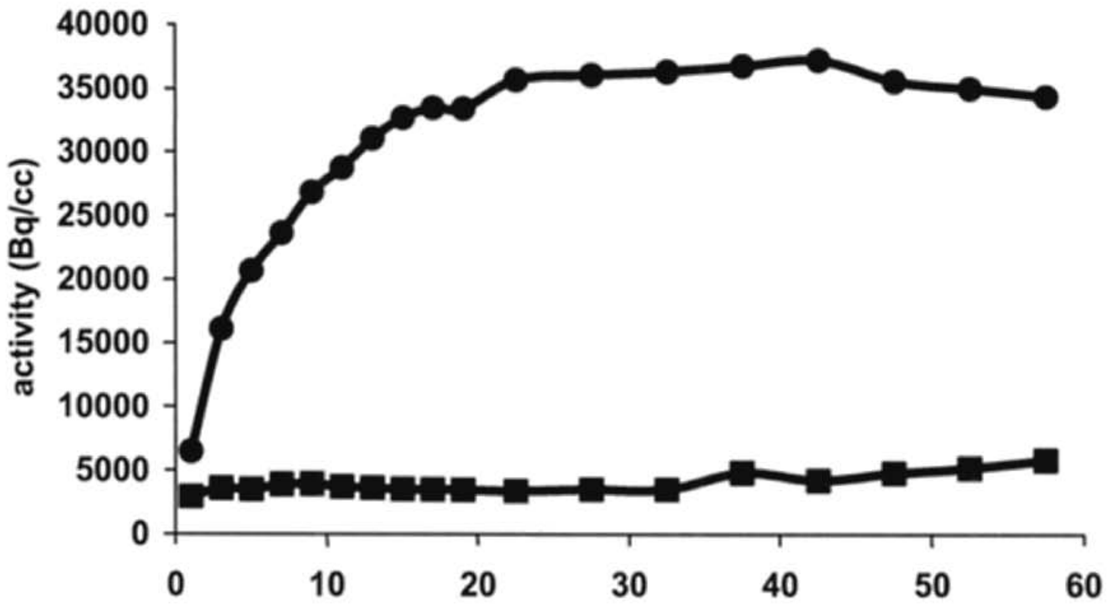

Fig. **3** Time-activity curves of 2-[^{18}F]fluoroethoxy-5-bromoglibenclamide distribution in a healthy volunteer. Curves shows high uptake of the tracer in the liver (black circles) and low uptake in the pancreas (black squares).

Discussion

For establishing a positron emission- or single photon emission tomography based PICM quantitation technique, it is necessary to find a suitable target located at the plasma membrane of the pancreatic islet cells and to synthesise a radioactively labelled ligand that binds with high affinity and specificity to this target. The selected target should have several characteristics: It should be exclusively expressed by the pancreatic islet cells but not by the exocrine pancreas and it should be present in a sufficient amount to guarantee a high signal density. Therefore, we focused our attention on human sulfonylurea receptor 1 (SUR1), which is located at the internal face of the plasma membrane of the pancreatic islet cells (Schwanstecher et al., 1994; Uhde et al., 1999) with approximately 5000 sulfonylurea high-affinity binding sites per cell (Niki et al., 1989). Due to the fact that glibenclamide strongly stimulates insulin release from the β-cells in humans by binding to this receptor, we focussed our attention on the synthesis and evaluation of a fluorine-18- or ^{99m}Tc-labelled glibenclamide derivative as possible ligand. After intravenous application, the fluorine-18- or ^{99m}Tc-labelled glibenclamide derivative should cross the plasma membrane and accumulate at their internal face where the SUR1 is located thus enabling the radioactive signal to be estimated non-invasively using PET- or SPECT-technique.

In recent years, several radioactive molecules have been used for assessment of PICM *in vitro* or in animal models. For example, Moore et al. (2001) used a [^{111}In]indium labelled IC2 antibody specific for a cell surface antigen of pancreatic β-cells, which showed a direct correlation between accumulation of the tracer and the β-cell mass in a mouse model. But due to open questions concerning the exact localization of the IC2 antigen, its metabolism and labelling the tracer with indium instead of ^{99m}Tc the authors concluded that more work and a modification of the tracer is needed before practical clinical application is possible. Recently Sweet et al. (2004) made a systematic screening of potential β-cell imaging agents such as tolbutamide, serotonin, L-DOPA, dopamin, nicotinamide, fluorodeoxyglucose, and fluorodithizone and concluded that none of these compounds were likely candidates providing sufficient specificity for quantification with PET. Furthermore, Ladriere et al. (2001) showed that a [^{125}I]iodine-labelled mouse monoclonal antibody directed against a β-cell surface ganglioside was also not a promising tool for β-cell imaging *in vivo* as it lacked a specific uptake into the endocrine pancreas. Ladriere et al. (2000) showed also for tritiated glibenclamide that no significant difference in the paired ratio between the radioactive content of the pancreas and plasma could be found between control and diabetic rats. But in contrast to this we used a ^{18}F- and a ^{99m}Tc-labelled glibenclamide derivative for our *in vivo* evaluation. Labelling with fluorine-18 or ^{99m}Tc leads to structural modifications of the compound with possible alterations of the *in vitro* and *in vivo* behaviour. Therefore, the results obtained by Ladriere et al. (2000) can only be partially compared with the data presented in this study.

As revealed by our *in vitro* studies the introduction of fluorine or RE (as non-radioactive analogue to ^{99m}Tc) into the glibenclamide molecule leads to only slight variations of its binding affinity to human SUR1 and the insulin stimulating capacity when compared to the original glibenclamide. In contrast to this, the lipophilicity of the derivatives was influenced in a more pronounced way, dependent on the structures that were introduced. For example the fluorine-labelled compounds 8, 12, and 16 were found to be much more lipophilic due to structural elements such as

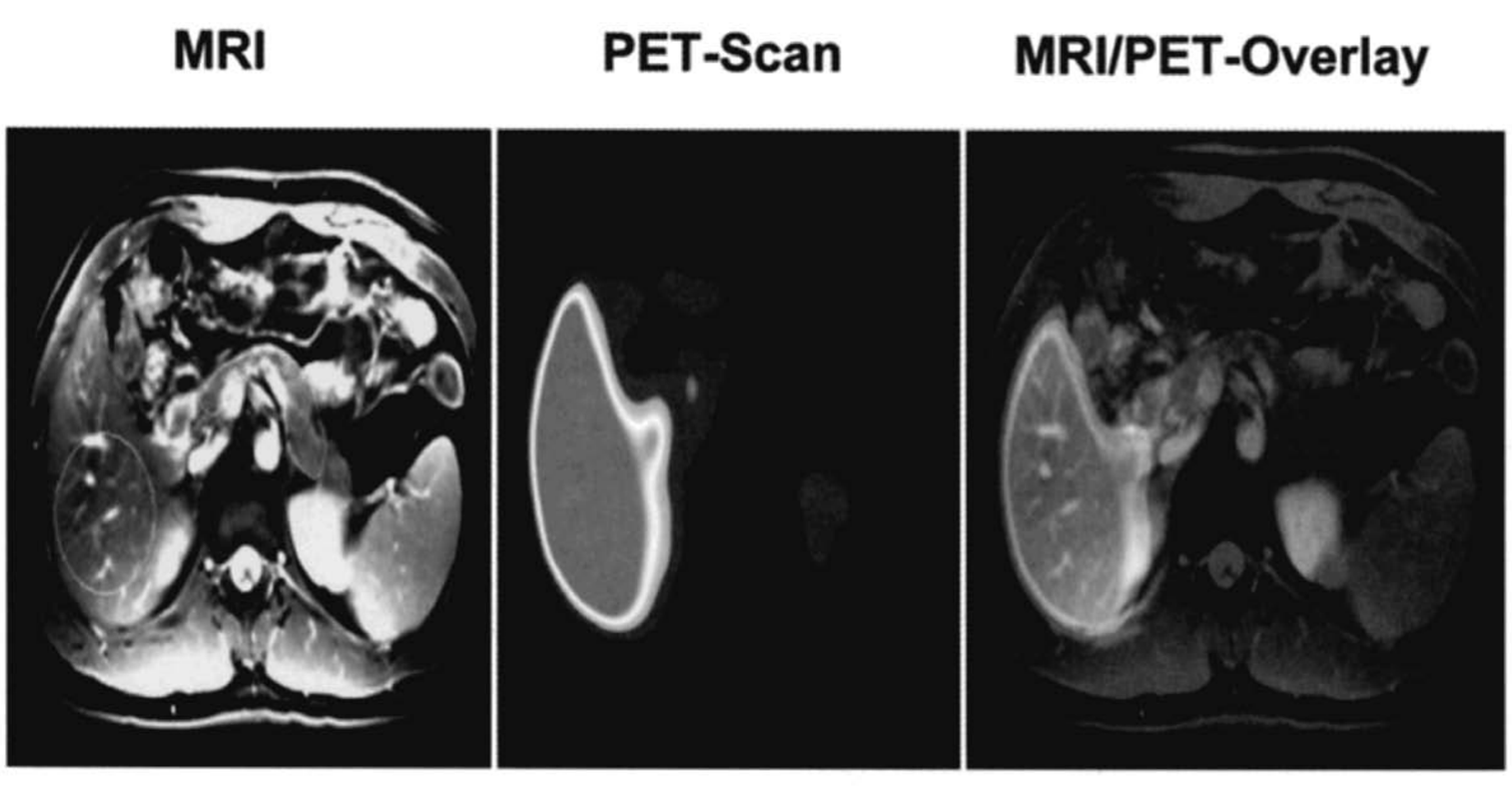

Fig. **4** MRI, PET-Scan, and MRI/PET-Overlay in a healthy volunteer. With magnetic resonance imaging (MRI), the liver and pancreas were easily detected. Afterwards, regions-of-interest (ROI) were manually drawn in the 3D MRI data and superimposed onto the realigned PET data. MRI/PET-Overlay shows high radioactive signal in the liver, but no visible radioactive signal in the pancreas.

the fluorobenzyl moiety and the chlorine, bromine, and iodine substituents. It is worth mentioning that lipophilic derivatives could show an unspecific uptake by various cell types and high plasma protein binding which could lead to the deterioration of the signal-to-noise ratio. But this has to be tested, because the lipophilicity seems not to be the only factor of influence (Wängler et al., 2004a, b). 2-[^{18}F]fluoroethoxy-5-bromoglibenclamide (compound 9, Table **1a**) was chosen for the first *in vivo* evaluation of a fluorine-18 labelled sulfonylurea, because the ligand shows high affinity binding to human SUR1, a relativley low logD indicating less lipophilicity than most of the other synthesised compounds and the radioactive label could be easily introduced. In the human PET-study a constant but weak radioactive signal could be detected in the pancreas (up to ten times less than the liver signal, Fig. **3**). These data fit quite well with the results from our *in vivo* study in rats. However, a reliable assessment and visualisation of the PICM could not be obtained with this tracer. It can be assumed that the high uptake of the tracer into the liver but also into other organs (e.g. kidney) and the high plasma protein binding, seen in the animal model as well as in both human volunteers, leads to a poor signal-to-noise ratio. In case of the presented fluorine-labelled glibenclamide based compounds this could be the result of their invariably high lipophilicity. Due to only slight differences concerning their *in vitro* characteristics, we would therefore expect that none of the presented fluorinated compounds (1 – 20) will be suitable for non-invasive imaging of the PICM. These results are in agreement with those obtained by others (Sweet et al., 2004; Hwang et al., 2003; Ladriere et al., 2000). For this reason, it is mandatory either to find a completely different tracer molecule (e.g. a radioactive labelled repaglinide derivative; Wängler et al., 2004a, b) or even to develop a glibenclamide derivative with significantly altered *in vitro* and *in vivo* characteristics. For this purpose, we synthesised a hydrophylic ^{99m}Tc- respectiveley analogous non-radioactive Re labelled glibenclamide derivative. This derivative showed a high binding affinity toward human SUR1 (K_D = 0.5 nM) and a well preserved insulin stimulating capacity, but an approximately 20-fold lower lipophilicity (logD = – 0.2) when compared to the fluorinated glibenclamide derivatives (1 – 20) or the original glibenclamide. Furthermore, after injection into euglycemic rats, liver uptake and plasma protein binding were three orders of magnitude lower than for the fluorine-18 glibenclamide derivative, whereas the pancreas uptake decreased 10-fold. So, the overall uptake of the ^{99m}Tc-labelled compound in the pancreas relative to other tissue compartments is more specific for pancreas by two orders of magnitude. These preliminary results are encouraging and it could be assumed that this will lead to an increased signal-to-noise ratio and a better detection of the pancreas signal. But more work is needed to prove if a ^{99m}Tc-labelled glibenclamide derivative will really be suitable for non-invasive imaging of the pancreatic islet cell mass.

In conclusion, we clearly showed that it is feasible to develop radiolabelled glibenclamide derivatives with high purity, acceptable radiochemical yield, a well preserved binding affinity toward human SUR1 and insulin stimulating capacity. However, neither the original glibenclamide as shown in the literature (Sweet et al., 2004; Hwang et al., 2003; Ladriere et al., 2000) nor fluorinated glibenclamide derivatives with nearly the same *in vitro* characteristics will allow the non-invasive imaging of the PICM. The development of a ^{99m}Tc-labelled glibenclamide derivative with a lower lipophilicity and differing *in vivo* behaviour, glibenclamide-based compounds for non-invasive imaging of the pancreatic islet cell mass may be possible.

Acknowledgements

We are indebted to Jupp Schlosser and Marcus Weiland for help in these experiments. The authors wish to thank Sabine Höhneman for the syntheses and quality control of 2-[^{18}F]fluoroethyltosylate and the ^{18}F-labelled glibenclamide. This work was supported by grants of the German Diabetes Association to S. S. and R. S., the Mainzer Forschungsförderung (MAIFOR 9728298) to P. J. F. and R. S., a grant donated by the Wissenschaftskommission of the University Hospital Bergmannsheil Bochum to S. S., the Bürger Büsing Stiftung, and financial support of Juvenile Diabetes Foundation International to CYS and AAA.

References

[1] Aguilar-Bryan L, Bryan J. Molecular biology of adenosine triphosphate-sensitive potassium channels. Endocr Rev 1999; 20: 101 – 135
[2] Bottino R, Lemarchand P, Trucco M, Giannoukakis N. Gene- and cell-based therapeutics for Type I diabetes mellitus. Gene Ther 2003; 10: 875 – 889
[3] Eadsforth CV, Moser P. Assessment of reverse-phase chromatographic methods for determining partition coefficients. Chemosphere 1983; 12: 1459 – 1475
[4] Eadsforth CV. Applications of reverse-phase h.p.l.c for the determination of partition coefficients. Pestic Sci 1986; 17: 311 – 325
[5] Hwang DR, Phan V, Huang Y, Laruelle M, Jerabek P, Fox P, De Fronzo R. Evaluation of [C-11]glyburide as a pancreatic beta-cell imaging agent. NIH Sponsored Workshop: Imaging the Pancreatic Beta Cell. April 21 – 22, 2003
[6] Ladriere L, Malaisse-Lagae F, Malaisse WJ. Uptake of tritiated glibenclamide by endocrine and exocrine pancreas. Endocrine 2000; 13: 133 – 136
[7] Ladriere L, Malaisse-Lagae F, Alejandro R, Malaisse WJ. Pancreatic fate of a (125)I-labelled mouse monoclonal antibody directed against pancreatic B-cell surface ganglioside(s) in control and diabetic rats. Cell Biochem Funct 2001; 19: 107 – 115
[8] Moore A, Bonner-Weir S, Weissleder R. Noninvasive in vivo measurement of beta-cell mass in mouse model of diabetes. Diabetes 2001; 50: 2231 – 2236
[9] Niki I, Kelly RP, Ashcroft SJ, Ashcroft FM. ATP-sensitive K-channels in HIT T15 beta-cells studied by patch-clamp methods, 86Rb efflux and glibenclamide binding. Pflugers Arch 1989; 415: 47 – 55
[10] Pietrzyk U, Herholz K, Heiss WD. Three-dimensional alignment of functional and morphological tomograms. J Comput Assist Tomogr 1990; 14: 51 – 59
[11] Pietrzyk U, Herholz K, Fink G, Jacobs A, Mielke R, Slansky I, Wurker M, Heiss WD. An interactive technique for three-dimensional image registration: validation for PET, SPECT, MRI and CT brain studies. J Nucl Med 1994; 35: 2011 – 2018
[12] Proks P, Reimann F, Green N, Gribble F, Ashcroft F. Sulfonylurea stimulation of insulin secretion. Diabetes 2002; 51: 368 – 376
[13] Schirrmacher R, Weber M, Schmitz A, Shiue SY, Alavi AA, Feilen PJ, Schneider S, Kann P, Rösch F. Radiosyntheses of 1-(4-{2-[^{18}F]fluoroethoxy}benzenesulfonyl)-3-butyl urea: A potential β-cell imaging agent. J Label Compd Radiopharm 2002; 45: 763 – 774
[14] Schneider S, Feilen PJ, Brunnenmeier F, Minnemann T, Zimmermann H, Zimmermann U, Weber MM. Long-term graft function of adult rat and human islets encapsulated in novel alginate-based microcapsules after transplantation in immunocompetent diabetic mice. Diabetes 2005; 54: 687 – 693
[15] Schneider S, Feilen PJ, Cramer H, Hillgartner M, Brunnenmeier F, Zimmermann H, Weber MM, Zimmermann U. Beneficial effects of human

serum albumin on stability and functionality of alginate microcapsules fabricated in different ways. J Microencapsulation 2003; 20: 627–636
16 Schwanstecher M, Brandt Ch, Behrends S, Schaupp U, Panten U. Effect of MgATP on pinacidil-induced displacement of Glibenclamide from the sulphonylurea receptor in a pancreatic β-cell line and rat cerebral cortex. Br J Pharmacol 1992; 106: 295–301
17 Schwanstecher M, Schwanstecher C, Dickel C, Chudziak F, Moshiri A, Panten U. Location of the sulphonylurea receptor at the cytoplasmic face of the beta-cell membrane. Br J Pharmacol 1994; 113: 903–911
18 Schwanstecher M, Sieverding C, Dorschner H, Gross I, Aguilar-Bryan L, Schwanstecher C, Bryan J. Potassium channel openers require ATP to bind to and act through sulfonylurea receptors. EMBO J 1998; 17: 5529–5535
19 Shiue GG, Schirrmacher R, Shiue CY, Alavi A. Syntheses of fluorine-18 labeled sulfonureas as β-cell imaging agents. J Label Compd Radiopharm 2001; 46: 959–977
20 Shiue CY, Schmitz A, Schirrmacher R, Shiue GG, Alavi AA. Potential approaches for β-cell imaging with PET and SPECT. Curr Med Chem-Immun Endoc & Metab Agents 2004; 4: 271–280
21 Sweet IR, Cook DL, Lernmark A, Greenbaum CJ, Wallen AR, Marcum ES, Stekhova SA, Krohn KA. Systematic screening of potential beta-cell imaging agents. Biochem Biophys Res Commun 2004; 314: 976–983
22 Uhde I, Toman A, Gross I, Schwanstecher C, Schwanstecher M. Identification of the potassium channel opener site on sulfonylurea receptors. J Biol Chem 1999; 274: 28079–28082
23 Wängler B, Shiue CY, Schneider S, Schwanstecher C, Schwanstecher M, Feilen PJ, Alavi A, Rösch F, Schirrmacher R. Synthesis and *in vitro* evaluation of (S)-2-([^{11}C]methoxy)-4-([3-methyl-1-(2-piperidine-1-yl-phenyl)-butyl-carbamoyl]-benzoic acid ([^{11}C]methyl-Repaglinide): a potential β-cell imaging agent. Bioorg Med Chem Lett 2004a; 14: 5205–5209
24 Wängler B, Schneider S, Thews O, Schirrmacher E, Comagic S, Feilen P, Schwanstecher C, Schwanstecher M, Shiue CY, Alavi A, Höhnemann S, Piel M, Rösch F, Schirrmacher R. Synthesis and evaluation of [^{18}F]repaglinide: a promising radioligand for quantification of pancreatic β-cell mass with positron emission tomography (PET). Nucl Med Biol 2004b; 31: 639–647

Novel Mutation (Gly280Ala) in the ATP-Binding Domain of Glycerol Kinase Causes Severe Hyperglycerolemia

T. Wibmer[1,2]
J. Otto[1,3]
K. G. Parhofer[2]
C. Otto[2]

Abstract

Glycerol kinase deficiency is a rarely diagnosed X-linked recessive disorder which occurs as a complex form together with the adrenal hypoplasia congenita (AHC) or with Duchenne muscular dystrophy (DMD) or as an isolated form either symptomatic or asymptomatic. We report the case of a male adult who had pseudo-hypertriglyceridemia (falsely elevated triglycerides of 552 mg/dl) refractory to lipid-lowering therapy for more than 15 years. Further investigations revealed an isolated, asymptomatic glycerol kinase deficiency. Using polymerase chain reaction and direct DNA sequencing, a novel missense mutation Gly280Ala in the Xp21.3 glycerol kinase gene was found. Comparison between human and E.coli glycerol kinase showed that the mutation affects a highly conserved amino acid in an ATP-binding domain in the active centre. This mutation is assumed to destabilize a hydrogen bond between ligand and enzyme resulting in a reduced activity of glycerol kinase and therefore in hyperglycerolemia.

Key words
GK · glycerol kinase · GKD · glycerol kinase deficiency · hyperglycerolemia

Introduction

Glycerol kinase (GK, Genbank accession number L13943 and X78211) catalyses the phosphorylation of glycerol with ATP to form glycerol-3-phosphate and ADP. Glycerol-3-phosphate is an important intermediate between glucose and lipid metabolism and may serve as substrate in a variety of pathways such as glycolysis, glycogenesis, the synthesis of triglycerides and other glycerolipids (Fig. **1**). Glycerol kinase is the key enzyme for glycerol's entry into metabolism. Loss of enzyme activity is therefore characterized by raised levels of free glycerol in both the serum (hyperglycerolemia) and the urine (hyperglyceroluria).

Glycerol kinase deficiency (GKD, MIM# 307030) is an X-linked recessive disorder and occurs in two distinct forms. The complex GKD is a contiguous gene deletion syndrome and involves deletions of the GK locus (GK gene) together with the Duchenne muscular dystrophy locus (DMD gene) or the adrenal hypoplasia congenita (AHC) locus (DAX1 gene) or both (Sjarif et al., 2000).

The isolated form of GKD results from either point mutations, small deletions, or insertions within the GK gene and is not associated with AHC or DMD. It can be either symptomatic or asymptomatic with hyperglycerolemia and glyceroluria only. The symptomatic form is characterized by Reye-like symptoms including episodic metabolic and central nervous system decompensation, mental retardation, and developmental delay (Sjarif

Affiliation
[1] Physiological Chemistry, Adolf Butenandt Institute, University of Munich, Germany
[2] Medical Department 2 – Großhadern, University Hospital Munich, Germany
[3] deceased

Correspondence
Carsten Otto, M.D. · Medical Department 2 – Großhadern · University Hospital of Munich · Marchioninistraße 15 · 81377 Munich · Germany · T + 49 89 7095 2268 or 7095 0 · F + 49 89 7095 8879 · E-mail: carsten.otto@med.uni-muenchen.de

Received: August 12, 2004 · **First decision:** October 22, 2004 · **Accepted:** April 13, 2005

Bibliography
Exp Clin Endocrinol Diabetes 2005; 113: 396 – 403 © J. A. Barth Verlag in Georg Thieme Verlag KG · Stuttgart · New York ·
DOI 10.1055/s-2005-865723 ·
ISSN 0947-7349